Journal of Environmental Chemical Engineering 8 (2020) 104105

Contents lists available at ScienceDirect

Journal of Environmental Chemical Engineering

journal homepage: www.elsevier.com/locate/jece

Diclofenac sorption from synthetic water: Kinetic and thermodynamic analysis

Stefano Salvestrini[a,b], Angelo Fenti[c], Simeone Chianese[b,c,*], Pasquale Iovino[a,b], Dino Musmarra[b,c]

[a] Department of Environmental, Biological and Pharmaceutical Sciences and Technologies, University of Campania "Luigi Vanvitelli", via Vivaldi 43, 81100 Caserta, Italy
[b] Environmental Technologies, University Spin Off of University of Campania "Luigi Vanvitelli", Via Vivaldi, 43, 81100 Caserta, Italy
[c] Department of Engineering, University of Campania "Luigi Vanvitelli", Via Roma 29, 81031 Aversa CE, Italy

ARTICLE INFO

Editor: GL Dotto

Keywords:
Diclofenac
Sorption
Kinetics
Thermodynamics
Emerging and refractory pollutants
Exothermic sorption

ABSTRACT

This work investigated diclofenac sorption on 0.5 g L^{-1} activated carbon in a range of temperature (288 – 318 K) and of initial sorbate concentration (24 – 218 mg L^{-1}). Thermodynamic modelling was carried out with the Langmuir isotherm. For kinetic modelling we compared the so-called Diffusion-Controlled Langmuir Kinetics (DCLK) and the pseudo-second order (PSO) model. The maximum sorption capacity of the sorbent, equal to 180 mg g^{-1}, was independent of temperature. Experimental data fitted well with both kinetic models, yet the DCLK model was found to be more informative about the mechanism of the process. Kinetic parameters (α, β) increased with the temperature, with α value rising from 5×10^{-5} to 20×10^{-5} L mg^{-1} $min^{-0.5}$, and β value rising from 3×10^{-6} to 20×10^{-6} L mg^{-1} min^{-1} in the temperature range investigated.

1. Introduction

More than 200 pharmaceutically active compounds (PhACs) of human origin, such as non-steroidal anti-inflammatory drugs, antibiotics and analgesics, are a common occurrence in environmental comparts including surface water, groundwater, sewage and soil [1,2]. The current understanding of long-term effects of these compounds on human health and ecosystem functionality is still incomplete, yet, their potential toxicity for freshwater aquatic organisms has been clearly established [3]. Moreover, reports of PhACs impairing the metabolic activity of soil microbial community have raised concern about ecological damage from the use of water from sewage treatment plants for irrigation and of biosolids and sludges for soil amendment [4].

Diclofenac (DCF), a non-steroidal anti-inflammatory drug of large use for therapy of inflammatory syndromes and painful conditions, is frequently detected in the environment [5]. The presence of DCF, and of its metabolite forms, in aquatic and soil comparts can be linked to a diversity of sources, such as domestic discharge or wastes from hospitals and pharmaceutical industries [5–7]. DCF toxicity for fish and insect species has been extensively investigated. It has been found, for example, that DCF caused vitellogenin expression in the males of medaka fish (*Oryzias latipes*) [8], and reduced the emergence rate of adults in the midge *Chironomus riparius* [9]. DCF was included in the Drinking Water Contaminant Candidate List and classified as class I, i.e. high-priority pharmaceutical products according to the Global Water Research Coalition [10]. DCF is also considered as an emerging contaminant and listed in the Watch List of EU Decision 2015/495 [11].

The global occurrence of diclofenac in a diversity of water bodies including surface water, seawater, groundwater, drinking water, and effluents from municipal wastewater treatment plants (MWWTP), was recently reviewed [5]. This study points to DCF contamination of surface water and seawater at concentrations in the range (order of magnitude) 1 ng L^{-1} - 10 µg L^{-1}, with the highest values of 57.16 µg L^{-1} and 10.2 µg L^{-1}, respectively. Diclofenac was detected in groundwater at concentrations in the range (order of magnitude) 10 ng L^{-1} - 10 µg L^{-1}, with a peak value of 13.48 µg L^{-1}. Drinking water showed a concentration of DCF in the range (order of magnitude) 1 ng L^{-1} - 10 ng L^{-1}, with the highest value of 56 ng L^{-1}. Diclofenac concentration in effluents from municipal wastewater treatment plants varied in the range (order of magnitude) 10 ng L^{-1} - 10 µg L^{-1}, with a peak value of 19 µg L^{-1}. These values clearly point to a low removal efficiency of conventional wastewater treatment processes for diclofenac, probably reflecting its resilience to biological depuration processes [10,12]. As a matter of fact, traditional treatment systems adopted in MWWTPs may increase DFC concentrations in the effluent [5,13].

Because of the above difficulties, the removal of DFC and other similarly refractory molecules requires the application of tertiary treatment methods, such as sorption [14–17] and Advanced Oxidation Processes (AOPs) [18–21]. AOPs, including photocatalysis with TiO_2 [22–24], photolysis [25–27], ozonation [28] and Fenton [29], showed

* Corresponding author at: Department of Engineering, University of Campania "Luigi Vanvitelli", Via Roma 29, 81031 Aversa CE, Italy.
E-mail address: simeone.chianese@unicampania.it (S. Chianese).

https://doi.org/10.1016/j.jece.2020.104105
Received 22 February 2020; Received in revised form 18 May 2020; Accepted 23 May 2020
Available online 03 June 2020

great potentiality in terms of concentration reduction, although the formation of potential harmful by-products has to be taken into account when oxidation techniques are used [30]. An alternative approach that does not involve harmful by-product generation, is the application of sorption techniques. A study of diclofenac removal from aqueous solution by sorption on lignite activated coke reported a maximum sorption capacity of 224 mg g^{-1} (Langmuir isotherm, T = 25 °C; pH = 6.5) [31]. Magnetic amine-functionalized chitosan displayed a maximum sorption capacity of 469.48 mg g^{-1} (Langmuir isotherm, T = 30 °C, pH = 4.5) [32]. An oxidized activated carbon displayed a maximum sorption capacity of 490 mg g^{-1} (Langmuir isotherm, T = 25 °C; pH = 5.5) has been reported for an oxidized activated carbon [33]. In all above-mentioned studies, the sorption process followed the pseudo-second-order kinetic model. Lonappan et al. [34] developed biochar-based green functional materials for diclofenac removal; starting from an initial concentration of DFC of 500 µg L^{-1}, they found a removal efficiency of 80 % and 84 % for pinewood biochar and almond shell biochar, respectively.

Diclofenac sorption can be strongly influenced by temperature [35]. An increase of the temperature is expected to cause an increase of sorption rate because of enhanced sorbate diffusion [36], although is some cases the opposite occurs [37]. On the other hand, the maximum sorption capacity can either increase or decrease depending on whether the sorption process is endo- or exothermic [38,39]. Therefore, assessing the effect of temperature on the kinetics and the thermodynamics of sorption is a crucial point for evaluating the efficiency of the process.

Here we report a study of the sorption of diclofenac from synthetic water onto 0.5 g L^{-1} commercial activated carbon in a range of temperature (288 − 318 K) and initial concentration of free sorbate (24 − 218 mg L^{-1}). Thermodynamic modelling was carried out with the Langmuir isotherm. Kinetic modelling was performed by comparing a hybrid kinetic model based on Langmuir surface reaction theory and Waite's theory of diffusion, known as Diffusion-Controlled Langmuir Kinetics (DCLK) [40], and the pseudo-second order (PSO) model [41]. The main thermodynamic parameters (standard change in Gibbs free energy, enthalpy and entropy) and the kinetic parameters were assessed.

2. Materials and methods

2.1. Materials

Sorption experiments were carried out by using a commercial activated carbon, Filtrasorb 400 (F400), from Calgon Carbon Corporation. This sorbent material is highly microporous, with a micropore volume equal to 0.31 $cm^3 g^{-1}$ and a BET surface area of about 1000 $m^2 g^{-1}$ [35]. A detailed description of its physical and chemical properties, including pore size distribution, acidic/basic surface functional groups, superficial chemical analysis and proximate analysis, has been reported elsewhere [42,43].

A diclofenac sodium salt (Na-DCF) of analytical grade with purity ≥ 98.5 % (CAS: 15307 − 79-6; Sigma-Aldrich, UK) was used to prepare experimental solutions in MilliQ water without further purification.

2.2. Determination of the point of zero charge

The zero charge pH (pH_{pzc}) of the sorbent was determined by pH titration [44,45]. Forty mL aliquots of 0.01 M NaCl solution were placed in 50 mL test tubes and the pH was adjusted to a value between 2 and 11 by adding few drops of 0.1 M HCl or 0.1 M NaOH solution. Twenty milligrams of F400 were added to each solution, and after 48 h the final pH (pH_{final}) was measured and plotted against the initial pH ($pH_{initial}$). The pH at which the curve pH_{final} vs $pH_{initial}$ crossed the line $pH_{final} = pH_{initial}$ gave the pH_{pzc} of F400.

2.3. Sorption experiments

Before use, the F400 was washed with milliQ water and dried in oven at 65 °C overnight, in order to remove impurities. The washing procedure was repeated three times.

All sorption experiments were carried out by batch method in pure water. Preliminary experiments in the presence of NaCl (10 mM, 50 mM or 100 mM) revealed that the ionic strength had a negligible effect on sorption. Five mg of F400 were transferred to 10 mL of DCF aqueous solution (24 − 218 mg L^{-1}) in 15 mL test tubes. The samples were incubated at different temperatures (15, 25, 35 and 45 °C) in a Benchmark Scientific MyTemp™ Mini Digital Incubator, under agitation speed of 30 rpm, for 120 h on a Benchmark Scientific Mini Nutating Rocker. At selected intervals, small aliquots of surnatant were analysed by UV–vis spectroscopy on a Perkin Elmer, Lambda 40, spectrometer, optical path = 0.1 − 1 cm. DCF concentration was assessed at 275 nm, following a previous method [46] and using the molar extinction coefficient of 0.0386 L cm^{-1} mg^{-1}.

The amount of DCF sorbed per mass of sorbent (q, expressed as mg g^{-1}) was determined from mass balance analysis:

$$q = \frac{C_0 - C}{X} \quad (1)$$

where C_0 and C represent the initial concentration and the concentration at any time t of DCF in the liquid phase, respectively, whereas X is the sorbent dosage, that is the mass of sorbent to the liquid volume ratio (g L^{-1}).

3. Results and discussion

3.1. Point of zero charge

DCF is a weak electrolyte characterized by an acid dissociation constant (pK_a) of 4.22 [47], with anionic and molecular forms coexisting in water solution in relative amounts depending on pH. At pH < 4.22, DCF mainly exists in the molecular form, at pH > 4.22 DCF the ionic form predominates.

The zero-charge pH of F400 is 6.5 (Fig. 1). Under the experimental conditions used (pH = 6.8 ± 0.2, either in the presence or in the absence of DCF), the sorbent surface is negatively charged and DCF is largely present in the anionic form, thus an electrostatic repulsion

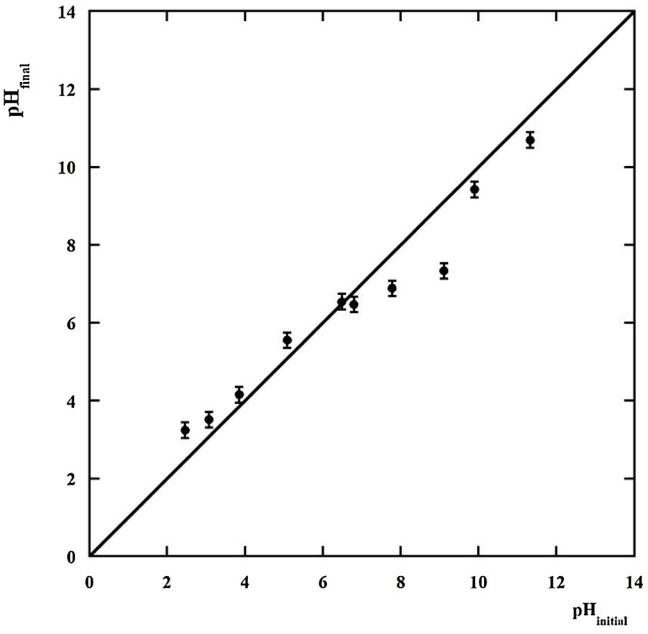

Fig. 1. Plot of the point of zero charge for F400.

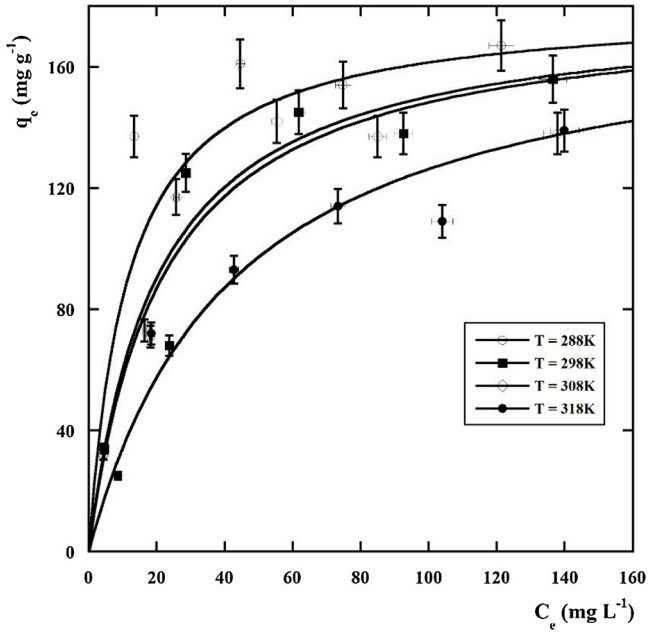

Fig. 2. Sorption isotherms of DCF onto F400; the curves in figure represent the isotherms predicted by the Langmuir model setting the maximum sorption capacity, q_m, as a shared fitting parameter.

occurs between DCF and the sorbent surface [48]. This also indicates that DCF sorption by F400 does not involve electrostatic attraction. Several other mechanisms are possible, such as π-π stacking, hydrogen bonding, hydrophobic–hydrophilic interactions and van der Waals forces [46,48–51].

3.2. Sorption thermodynamics

Fig. 2 shows the sorption isotherms of DCF onto F400 at different temperatures. The curves were obtained by least squares fitting of the Langmuir isotherm model ((Eq.2)) to the experimental data:

$$q_e = \frac{q_m K_L C_e}{1 + K_L C_e} \tag{2}$$

where q_e and C_e are the amount of DCF sorbed and the concentration of DCF in solution, respectively, at the equilibrium.

The fitting procedure was carried out by setting q_m as a shared parameter (as we have assumed that the availability of sorption sites does not vary with temperature). Numerical results of this calculation are reported in Table 1. The low error associated to the estimated value of q_m, of 180 mg g^{-1} suggests that the maximum sorption capacity of the sorbent is independent of temperature.

Table 2 is a survey of DCF sorption properties of different types of activated carbon, including maximum sorption capacities and operative conditions.

Table 1
Thermodynamic parameters for DCF sorption onto F400 as determined by the Langmuir isotherm model and by van't Hoff plot.

T (K)	q_m[a] (mg g^{-1})	$K_L \times 10^2$ (L mg^{-1})	$\Delta G°$[b] (kJ mol^{-1})	$\Delta H°$[b] (kJ mol^{-1})	$\Delta S°$[b] (J K^{-1} mol^{-1})
288.15	180 ± 10	8.7 ± 3.0	5.8	−29 ± 8	−122 ± 28
298.15		4.7 ± 0.9	7.6		
308.15		5.0 ± 0.8	7.7		
318.15		2.2 ± 0.5	10.1		

[a] Calculated by the Langmuir isotherm model using global fitting procedure.
[b] Selected standard states: 1 mg L^{-1} for the solute; 1 mg g^{-1} for the solid phase.

As shown, the values reported in the present manuscript are comparable with those reported in literature.

Table 1 also shows that the Langmuir equilibrium constant K_L has a decreasing trend with temperature. In order to obtain information on the thermodynamic parameters of sorption, namely the standard change in Gibbs energy ($\Delta G°$), enthalpy ($\Delta H°$) and entropy ($\Delta S°$), the following thermodynamic relationships were used [60]:

$$\Delta G° = -RTlnK_L \tag{3}$$

$$\Delta G° = \Delta H° - T\Delta S° \tag{4}$$

By combining Eqs. (3) and (4), one gets

$$lnK_L = -\frac{\Delta H°}{R}\frac{1}{T} + \frac{\Delta S°}{R} \tag{5}$$

Therefore, under the assumption that both $\Delta H°$ and $\Delta S°$ do not vary appreciably with temperature, a plot of lnK_L vs $1/T$ (van't Hoff plot) gives a straight line whose slope and intercept with y-axis, respectively, permit the determination of $\Delta H°$ and $\Delta S°$ (Fig. 3).

The numerical values obtained from the van't Hoff plot for $\Delta H°$ and $\Delta S°$ are −29 kJ mol^{-1} and −122 J K mol^{-1}, respectively (see also Table 1). The negative sign of $\Delta H°$ indicates that the sorption of DCF onto F400 is an exothermic process. A similar effect of temperature on the sorption of DCF was observed by De Oliveira et al. [61] using organoclays as sorbent materials in the temperature range 5 − 50 °C at pH 6.5, and by Lins et al. [62] using MgAl/LDH-activated carbon composite in the temperature range 30 − 60 °C at pH 5.5. In contrast, Suriyanon et al. [63] investigated the effect of temperature (T = 15 − 40 °C; pH 7) on DCF sorption from water solution by powdered activated carbon, and found that the sorption process was endothermic. Similar results were found by Tam et al. [64], who investigated the removal of DCF from aqueous solution by potassium ferrate-activated porous graphitic biochar in the temperature range 25 − 45 °C at pH = 6.5.

Table 1 shows values of $\Delta G° > 0$. Obviously, in no way does this result imply that the sorption process is not spontaneous. The sign of $\Delta G°$ must be not confused with that of ΔG, as often erroneously done in the literature [63]. The sign of $\Delta G°$ may merely depend on the selected standard state [65–67]. In our case, for example, a $\Delta G° < 0$ would have been obtained by expressing solute concentration as g L^{-1} instead of mg L^{-1}.

3.3. Effect of the initial aqueous concentration of DCF on the sorption kinetics

Fig. 4 shows the results of sorption experiments of DCF onto F400 at different initial concentrations of sorbate. A rapid uptake of DCF is observed in the first hours of the experiments, followed by a much slower phase leading to the equilibrium in about five days.

The data presented in Fig. 4 were preliminary analysed by the pseudo-second order (PSO) model [41], which is widely used for describing sorption kinetics in liquid/solid systems [68–73]. The PSO model is generally applied in its non-linear (hyperbolic) form (Eq.(6)) or linearized from (Eq.(7)):

$$q = \frac{q_e^2 k_{PSO} t}{1 + q_e k_{PSO} t} \tag{6}$$

$$\frac{t}{q} = \frac{t}{q_e} + \frac{1}{q_e^2 k_{PSO}} \tag{7}$$

Here k_{PSO} is the observed kinetic rate constant of the PSO model. In this work, the non-linear form of the PSO model (Eq.(6) was preferred for modelling the experimental data, as it provides a more correct estimate of the model parameters [74–76]. The results of the fitting procedure are displayed in Fig. S1 and in Table 3.

The PSO model described fairly well the kinetic profiles, suggesting that the rate of DCF sorption be proportional to the square of the

Table 2
DCF sorption properties of different types of activated carbon.

Sorbent material	Operative conditions	Diclofenac equilibrium concentration (C_e)	Equilibrium sorption capacity $q_e(C_e)$	Max removal efficiency	Reference
ACF	ACF dosage = 0.1 g L^{-1}; pH = 6.5; temperature = 25 °C	0.001 mM 0.015 mM	0.15 mmol g^{-1} 0.95 mmol g^{-1}	–	[52]
GAC	GAC dosage = N.A.; pH = 7.98; temperature = 30 °C	0.001 mM 0.25 mM	0.08 mmol g^{-1} 0.21 mmol g^{-1}	–	[53]
PAC	PAC dosage = N.A.; pH = 7.98; temperature = 30 °C	0.001 mM 0.20 mM	0.15 mmol g^{-1} 0.44 mmol g^{-1}		
AC	AC amount = 5 mg; Volume = 50 mL; pH = 5.4; temperature = 25 °C	1 ppm 90 ppm	3.3 mg g^{-1} 63 mg g^{-1}	–	[54]
AC	AC amount = 5 mg; Volume = 25 mL; pH = 5.5; temperature = 25 °C	18 ppm 88 ppm	30 mg g^{-1} 65 mg g^{-1}	–	[33]
PAC	PAC amount = 0.05 − 0.25 g; Volume = 50 − 500 mL; pH = 6; temperature = 25 °C	10 mg L^{-1} 242 mg L^{-1}	100 mg g^{-1} 323 mg g^{-1}	–	[55]
GAC	GAC amount = 0.05 − 0.25 g; Volume = 50 − 500 mL; pH = 6; temperature = 25 °C	0.5 mg L^{-1} 168 mg L^{-1}	10 mg g^{-1} 49.5 mg g^{-1}	63%	
PAC	PAC dosage = 10 mg L^{-1}; pH = 8; temperature = 20 °C	0.5 µg L^{-1}[a,d] 8 µg L^{-1}[a,d] 28 µg L^{-1}[b,d] 42 µg L^{-1}[b,d]	1 µg g^{-1}[o] 4.2 µg g^{-1}[o] 0.5 µg g^{-1}[o] 1 µg g^{-1}[o]	97 % 27 %	[56]
PAC	PAC dosage = 10–20 mg L^{-1}; temperature = 20 °C	1197 ng L^{-1}[b]	N.A.	69 %	[57]
GAC	GAC dosage = 30–100 mg L^{-1}	287 ng L^{-1}[b]	7.5 µg g^{-1}[c]	93 %	[58]
PAC	PAC dosage = 30–100 mg L^{-1}		7.7 µg g^{-1}[c]	95 %	
PAC	PAC dosage = 50 mg L^{-1}	0.07 µg L^{-1}[b]	N.A.	30 %	[59]
GAC	GAC dosage = 0.5 g L^{-1}; pH = 6.8; temperature = 25 °C	5 mg L^{-1} 100 mg L^{-1}	35 mg g^{-1} 150 mg g^{-1}	81 %	This study

ACF = activated carbon fiber.
GAC = granular activated carbon.
PAC = powdered activated carbon.
AC = activated carbon.
N.R. = not reported.
N.A. = not available.
[a] Initial concentration in simulated municipal wastewater.
[b] Initial concentration in real municipal wastewater.
[c] Specific Sorption Capacity.
[d] Sorption pseudo-isotherms after 30 min of contact.

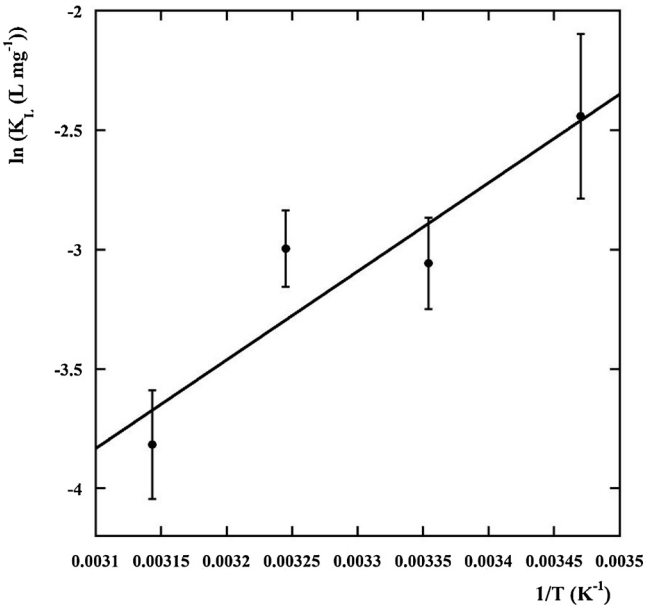

Fig. 3. van't Hoff plot for the sorption of DCF onto F400.

distance from equilibrium, $q_e - q$ [72]. Regression analysis gave a reliable estimate (low standard error) of k_{PSO}, whose value generally decreased with increasing C_0.

Although the fitting procedure was satisfactory, it should be noted that the PSO equation is a purely descriptive (empirical) model, hence the values of k_{PSO} at different C_0 are not interrelated and do not provide

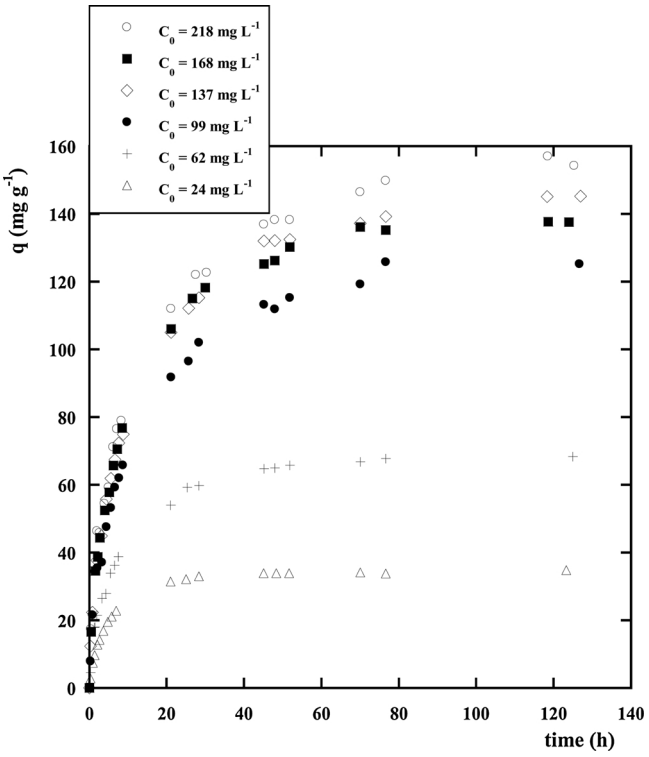

Fig. 4. Kinetic profiles of DCF sorption onto F400 at different initial solute concentrations; T = 25 °C, sorbent dosage = 0.5 g L^{-1}.

Table 3
PSO and DCLK model parameters for DCF sorption onto F400 at 25 °C; sorbent dosage = 0.5 g L^{-1}.

PSO model parameters					
C_0 (mg L^{-1})	q_e[a] (mg g^{-1})	$k_{PSO} \times 10^5$ (g mg^{-1} min^{-1})	Adj. R^2	RMSE	AIC
62	68 ± 8	5.1 ± 0.5	0.99	4.8	317
99	125 ± 15	2.0 ± 0.1			
137	145 ± 17	1.7 ± 0.1			
168	138 ± 17	2.0 ± 0.1			
218	156 ± 19	1.5 ± 0.1			

DCLK model parameters							
C_0 (mg L^{-1})	q_e[a] (mg g^{-1})	q_m[b] (mg g^{-1})	α[c] $\times 10^5$ (L mg^{-1} $min^{-0.5}$)	β[c] $\times 10^6$ (L mg^{-1} min^{-1})	Adj. R^2	RMSE	AIC
62	68 ± 8	180 ± 10	4.4 ± 0.5	4.6 ± 0.5	0.97	7.5	399
99	125 ± 15						
137	145 ± 17						
168	138 ± 17						
218	156 ± 19						

[a] Calculated from the plateau level of the kinetic profiles reported in Fig. 4.
[b] Calculated by the Langmuir isotherm model using global fitting procedure.
[c] Calculated by the DCLK model using global fitting procedure.

any information about the mechanism of the sorption process. To this end, alternative models need to be used.

In order to correctly interpret the data in figure and to gain insight on the mechanism of DCF sorption onto F400, it is important to take into account the possible effect of the microporosity of the sorbent material on the rate of the process. The rate of sorption is expected to be slowed down by diffusion phenomena because active sorbent sites mostly lie inside the sorbent particles, so that sorbable molecules have to diffuse through the pores of the sorbent, a process commonly known as intraparticle diffusion. A convenient method to assess whether the rate of sorption of DCF is affected by intraparticle diffusion, is to plot the sorbed amount q as a function of the square root of time. According to Crank diffusion theory [77], the linearity of this plot at an early stage of reaction is indicative of a sorption process governed by diffusion.

The plots of q vs $\sqrt{t}$ for the sorption of DCF onto F400 are reported in Fig. 5. As can be seen, an excellent linear correlation between the sorbed amount and $\sqrt{t}$ is obtained for small values of time, thus providing evidence that diffusion is the major driver of DCF sorption kinetics.

Taking into account the likely role of intraparticle diffusion, DCF sorption by F400 may be described as the sum of two reversible steps:

$$DCF + i \rightleftarrows_{k_{-D}}^{k_D} DCF\cdots i \rightleftarrows_{k_d}^{k_a} DCF - i \quad (8)$$

Here, k_D and k_{-D} are the diffusion rate constants for the formation and dissociation of the encounter complex (DCF···i) between DCF in solution and the sorption site i, and k_a and k_d are the microscopic kinetic rate constants for solute sorption and desorption, respectively.

The overall (net) rate of sorption, dθ/dt, for the reaction in Eq.(8) can be written as:

$$\frac{d\theta}{dt} = v_f - v_r = v_f\left(1 - \frac{v_r}{v_f}\right) \quad (9)$$

Here θ is the surface coverage fraction, i.e. the ratio between the sorbent amount q at any time and the maximum sorption level q_m; v_f and v_r are the overall forward and reverse rate of the process.

Assuming that the surface reaction is described by the Langmuir kinetics [78], Eq.(9) can be re-written as

$$\frac{d\theta}{dt} = v_f\left(1 - \frac{\theta}{C(1-\theta)}\frac{1}{K_L}\right) \quad (10)$$

where K_L is the Langmuir equilibrium constant.

Moreover, assuming that the overall rate of the process (Eq.(8)) is entirely controlled by diffusion, and considering that sorption is a bimolecular reaction, we may express the overall forward rate v_f of Eq. (10), in line with Waite's theory [40,79,80], as:

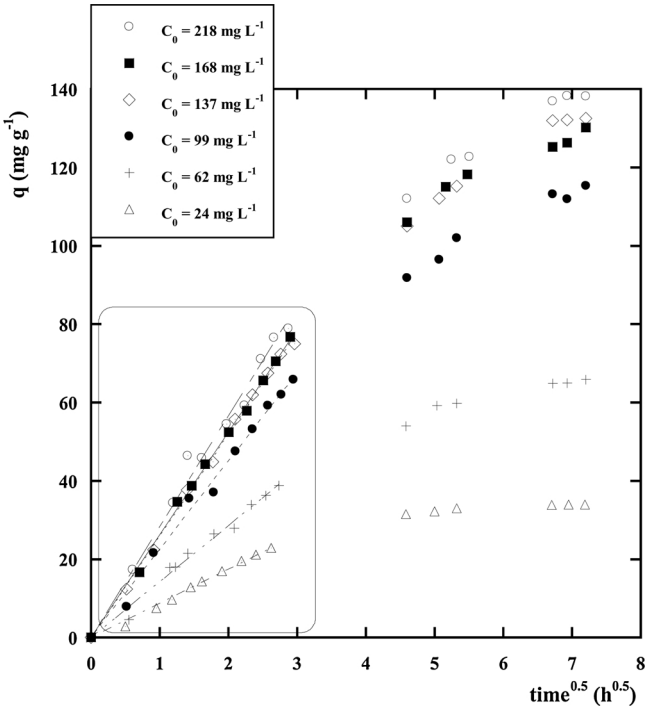

Fig. 5. Dependence of the sorbed amount q on the square root of time. The curves represent least squares lines forced through the origin.

$$v_f = \left(\frac{\alpha}{\sqrt{t}} + \beta\right)C(1-\theta) \quad (11)$$

$$\alpha = 4\frac{N_A}{M_w}r_0^2\sqrt{\pi D} \quad (12)$$

$$\beta = 4\frac{N_A}{M_w}r_0\pi D \quad (13)$$

Here N_A and M_w are the Avogadro number and the molecular weight of DCF, respectively; r_0 is the separation distance between DCF and any

site i suitable for sorption, and D is the *effective* diffusion coefficient of the DCF, i.e. the molecular diffusion coefficient corrected for the porosity of the sorbent.

Substituting Eq.(11) into Eq.(10) and integrating yields to:

$$q = q_e \frac{1 - exp[X(q_e - q_2)(2\alpha\sqrt{t} + \beta t)]}{1 - \frac{q_e}{q_2} exp[X(q_e - q_2)(2\alpha\sqrt{t} + \beta t)]} \quad (14)$$

$$q_2 = \frac{q_m C_0}{q_e X} \quad (15)$$

Eq.(14) represents a Diffusion-Controlled Langmuir Kinetics (hereafter referred to as DCLK) based on Waite's theory. Details on DCLK model derivation can be found in a previous report [40].

Eq.(14) was used to fit the data of Fig. 4. Notably, Eq.(14) contains four fitting parameters, namely the sorbed amount at equilibrium q_e, the maximum sorption capacity q_m, and the two kinetic parameters α and β. Of these, q_m, α and β are parameters common to all kinetic runs whereas q_e varies with experimental conditions (C_0 and X). Given that, reliable values of the unknown parameters can be obtained by performing a global fitting analysis of experimental data in which q_m, α and β are set as shared parameters, whilst q_e is calculated individually for each experimental data set. In order to simplify the fitting procedure, the number of adjustable parameters can be significantly reduced by using the values of q_e and q_m obtained from the plateau levels in Fig. 4 and from the Langmuir isotherm, respectively.

The results of the fitting procedure for the kinetic data reported in Fig. 4 are displayed in Fig. 6 and Table 2.

As can be seen from the figure, the DCLK model describes fairly well all the kinetic data set, with the exception of the set associated with the lowest solute concentration (24 mg L^{-1}), which was therefore excluded from global fitting calculation. The estimated values of α and β (see Table 2) are 4.4 × 10^{-5} L mg^{-1} $min^{-0.5}$ and 4.6 × 10^{-6} L mg^{-1} min^{-1}, respectively. The DCLK model and the PSO model were compared for goodness of fit using adjusted coefficient of determination (adj. R^2), root mean square error (RMSE) and Akaike's information criterion (AIC) [81]. The fitting results using the DCLK model are reasonably good (adj. R^2 = 0.97), although not as good as that obtained with the PSO model. Indeed, as can be seen from Table 2, the PSO model has higher adj. R^2, and lower RMSE and AIC values. Obviously, much better fitting results with the DCLK model could have been achieved by decreasing the constraints on the adjustable parameters, i.e. without parameters sharing (see Fig.S2), as in the case of the PSO model; the parameters so obtained, however, would have little bearing on the understanding of the sorption mechanism.

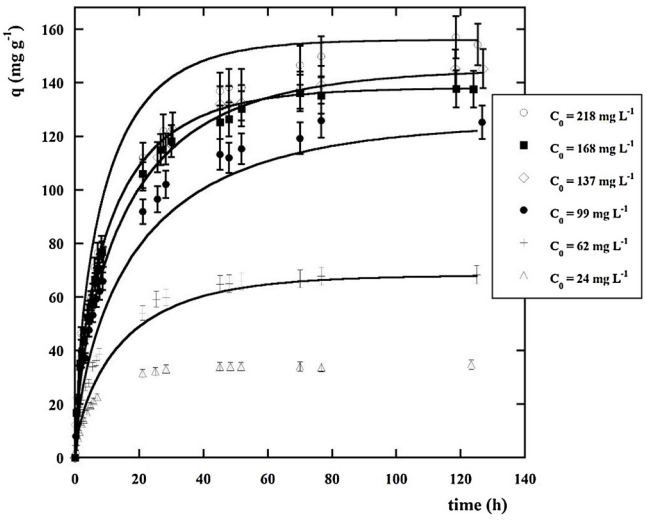

Fig. 6. Global fitting analysis of DCF sorption kinetic data at T = 25 °C setting α and β as shared parameters; sorbent dosage = 0.5 g L^{-1}.

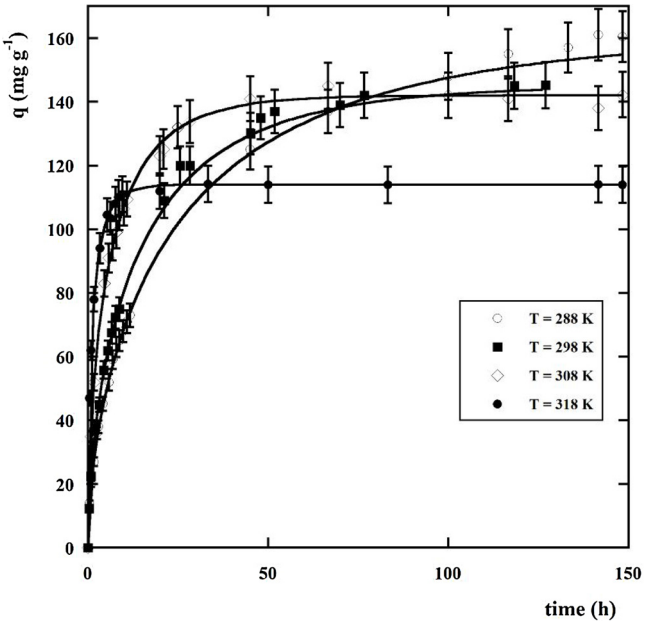

Fig. 7. Temperature effect on DCF sorption kinetics; C_0 = 140 mg L^{-1}, sorbent dosage = 0.5 g L^{-1}. The curves in figure represent the kinetics predicted by the DCLK model.

It is worth noting that in spite of lower fitting performance vs. the PSO model, the DCLK model has a great practical advantage over this and other empirical models. As a matter of fact, besides providing a description of actual experimental data, the DCLK model allows one to *predict* the kinetic behaviour of the sorbate (under varying operative conditions such as C_0, X and, as we will see below, temperature) on the basis of the estimated parameters related to the sorbate/sorbent interaction (sorbate diffusivity and sorbate/sorbent affinity).

3.4. Effect of temperature on the sorption kinetics

Fig. 7 shows the kinetic profiles of the sorption experiments at different temperatures. The data clearly show that the rate of sorption increases with temperature. In contrast, it is interesting to note a negative effect of temperature on the sorbed amount at equilibrium (plateau level of the kinetic data set). This latter finding, in line with the results of Fig. 2, reflects the exothermic nature of the process.

The curves in Fig. 7 represent the results of data fitting with the DCLK model (Eq.(14)). In order to correctly interpret the effect of temperature on the sorption rate, α and β were not set as shared parameters during the fitting procedure. The DCLK model adequately described the experimental data. The estimated values of α and β are reported in Table 4.

Both α and β values increase with temperature and, more interestingly, the increment of α is less than that of β, that is the β/α ratio increases with temperature. This behaviour appears to be fully consistent with the physical meaning of α and β parameters (see Eqs.(12) and (13)), most likely reflecting the dependence of diffusion rate on temperature:

$$\frac{\beta}{\alpha} = \frac{\sqrt{\pi D}}{r_0} \quad (16)$$

The role of diffusion in the sorption kinetics can be evaluated from the magnitude of the activation energy (E_a) obtainable from the Arrhenius law [82]:

$$D = D_0 e^{-\frac{E_a}{RT}} \quad (17)$$

Table 4
DCLK model parameters for DCF sorption onto F400 at different temperatures and related activation energy (E_a); sorbent dosage = 0.5 g L^{-1}, initial solute concentration = 140 mg L^{-1}.

T (K)	q_e[a] (mg g^{-1})	q_m[b] (mg g^{-1})	$\alpha \times 10^5$ (L mg^{-1} $min^{-0.5}$)	$\beta \times 10^6$ (L mg^{-1} min^{-1})	Adj. R^2	E_a (kJ mol^{-1})
288.15	161	180 ± 10	5.0 ± 0.4	3.1 ± 0.2	0.999	26 ± 8
298.15	145		5.9 ± 0.4	4.5 ± 0.4		
308.15	142		10 ± 1	8.9 ± 0.8		
318.15	114		20 ± 2	20 ± 1		

[a] Calculated from the plateau level of the kinetic profiles reported in Fig. 7.
[b] Calculated by the Langmuir isotherm model using global fitting procedure.

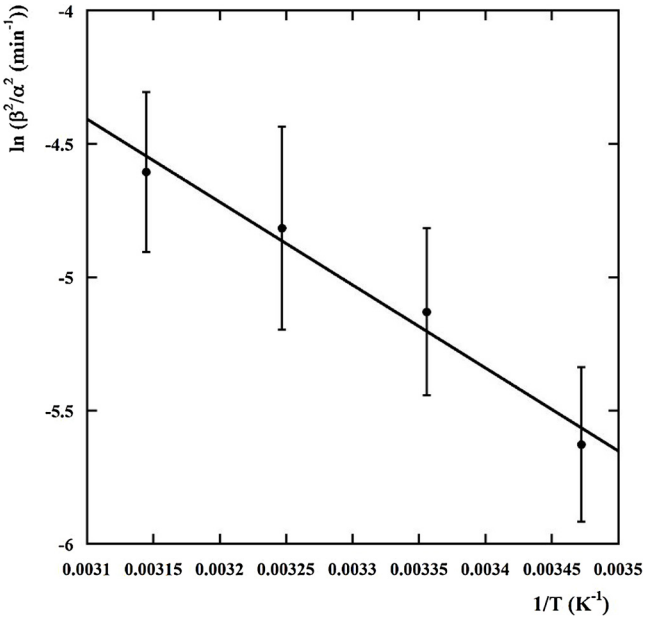

Fig. 8. Arrhenius plot for DCF sorption kinetics.

where D_0 is the Arrhenius pre-exponential factor, a temperature-independent parameter.

According to Eq.(17), a plot of ln$D$ vs $1/T$ should produce a straight line with slope equal to $-E_a/R$. Because β^2/α^2 is proportional to D, the β^2/α^2 ratio can be used in place of D in the Arrhenius plot to determine the slope of the line. The plot of $\ln\beta^2/\alpha^2$ vs $1/T$ for DCF sorption onto F400 (Fig. 8) shows a satisfying linear correlation (R^2 = 0.99) between $\ln\beta^2/\alpha^2$ and $1/T$. The activation energy determined from the slope of the line is E_a = 26 ± 8 kJ mol^{-1}. Within the experimental error, this value is consistent with values expected for diffusion-controlled sorption processes ($E_a \leq$ 20 kJ mol^{-1} [83]), thus reinforcing the conclusion that the DCLK model is the best choice for describing the sorption kinetics of DCF onto F400.

4. Conclusions

This study was mainly focused on kinetic and thermodynamic modelling of diclofenac sorption by F400. The Langmuir isotherm is a satisfactory thermodynamic model. The Diffusion-Controlled Langmuir Kinetics, a hybrid kinetic model based on the Langmuir surface reaction theory and on Waite's theory of diffusion, was found to be preferable to the pseudo-second order model for describing the kinetics of the process, because experimental evidence suggested that DCF sorption was controlled by intraparticle diffusion. Investigations were carried out by varying temperature (15 − 45 °C) and initial concentration of DCF (24 − 218 mg L^{-1}), and keeping constant the sorbent material concentration (0.5 g L^{-1}). Experimental findings highlighted that the maximum sorption capacity of the sorbent, equal to 180 mg g^{-1}, was independent of temperature. The Langmuir equilibrium constant decreased with increasing temperature from 8.7×10^{-2} to 2.2×10^{-2} L mg^{-1}, pointing out the exothermicity of the process.

Despite the PSO model showed better fitting (DCLK Adj R^2 = 0.97, RMSE = 7.5, AIC = 399; PSO Adj R^2 = 0.99, RMSE = 4.8, AIC = 317), the DCLK model was considered the best choice as it not only fitted well the experimental data but also provided predictive information on the sorbate behaviour. The kinetic parameters α and β linearly increased from 5×10^{-5} to 20×10^{-5} L mg^{-1} $min^{-0.5}$, and from 3×10^{-6} to 20×10^{-6} L mg^{-1} min^{-1}, respectively, with the temperature rising from 288 to 318 K.

CRediT authorship contribution statement

Stefano Salvestrini: Conceptualization, Writing - original draft. **Angelo Fenti:** Investigation. **Simeone Chianese:** Writing - review & editing. **Pasquale Iovino:** Data curation, Methodology. **Dino Musmarra:** Supervision.

Declaration of Competing Interest

The authors declare that they have no known competing financial interests or personal relationships that could have appeared to influence the work reported in this paper.

Acknowledgment

This work has been supported by VALERE "*VAnviteLli pEr la RicErca*" PROGRAMME funded by the University of Campania "Luigi Vanvitelli". The authors thank to Prof. Roberto Ligrone and Prof. Sante Capasso for the most useful discussion of the data.

Appendix A. Supplementary data

Supplementary material related to this article can be found, in the online version, at doi:https://doi.org/10.1016/j.jece.2020.104105.

References

[1] B. Petrie, R. Barden, B. Kasprzyk-Hordern, A review on emerging contaminants in wastewaters and the environment: current knowledge, understudied areas and recommendations for future monitoring, Water Res. 72 (2015) 3–27, https://doi.org/10.1016/j.watres.2014.08.053.
[2] C.F. Couto, L.C. Lange, M.C.S. Amaral, Occurrence, fate and removal of pharmaceutically active compounds (PhACs) in water and wastewater treatment plants—a review, J. Water Process Eng. 32 (2019) 100927, , https://doi.org/10.1016/j.jwpe.2019.100927.
[3] P. Amoatey, M.S. Baawain, Effects of pollution on freshwater aquatic organisms, Water Environ. Res. 91 (2019) 1272–1287, https://doi.org/10.1002/wer.1221.
[4] M.R. Pino-Otín, S. Muñiz, J. Val, E. Navarro, Effects of 18 pharmaceuticals on the physiological diversity of edaphic microorganisms, Sci. Total Environ. 595 (2017) 441–450, https://doi.org/10.1016/j.scitotenv.2017.04.002.
[5] P. Sathishkumar, R.A.A. Meena, T. Palanisami, V. Ashokkumar, T. Palvannan, F.L. Gu, Occurrence, interactive effects and ecological risk of diclofenac in environmental compartments and biota - a review, Sci. Total Environ. 698 (2020) 134057, , https://doi.org/10.1016/j.scitotenv.2019.134057.
[6] S. Schmidt, H. Hoffmann, L.A. Garbe, R.J. Schneider, Liquid chromatography–tandem mass spectrometry detection of diclofenac and related compounds in water samples, J. Chromatogr. A 1538 (2018) 112–116, https://doi.org/10.

1016/j.chroma.2018.01.037.
[7] V. Osorio, M. Imbert-Bouchard, B. Zonja, J.L. Abad, S. Pérez, D. Barceló, Simultaneous determination of diclofenac, its human metabolites and microbial nitration/nitrosation transformation products in wastewaters by liquid chromatography/quadrupole-linear ion trap mass spectrometry, J. Chromatogr. A 1347 (2014) 63–71, https://doi.org/10.1016/j.chroma.2014.04.058.
[8] C. Lacey, S. Basha, A. Morrissey, J.M. Tobin, Occurrence of pharmaceutical compounds in wastewater process streams in Dublin, Ireland, Environ. Monit. Assess. 184 (2012) 1049–1062, https://doi.org/10.1007/s10661-011-2020-z.
[9] E. Nieto, C. Corada-Fernández, M. Hampel, P.A. Lara-Martín, P. Sánchez-Argüello, J. Blasco, Effects of exposure to pharmaceuticals (diclofenac and carbamazepine) spiked sediments in the midge, Chironomus riparius (Diptera, Chironomidae), Sci. Total Environ. 609 (2017) 715–723, https://doi.org/10.1016/j.scitotenv.2017.07.171.
[10] P. De Voogt, M.L. Janex-Habibi, F. Sacher, L. Puijker, M. Mons, Development of a Common Priority List of Pharmaceuticals Relevant for the Water Cycle, (2009), https://doi.org/10.2166/wst.2009.764.
[11] K. Vella, Commission Implementing Decision (EU) 2015/495, (2015).
[12] J.L. Zhou, Z.L. Zhang, E. Banks, D. Grover, J.Q. Jiang, Pharmaceutical residues in wastewater treatment works effluents and their impact on receiving river water, J. Hazard. Mater. 166 (2009) 655–661, https://doi.org/10.1016/j.jhazmat.2008.11.070.
[13] T. Manickum, W. John, Occurrence, fate and environmental risk assessment of endocrine disrupting compounds at the wastewater treatment works in Pietermaritzburg (South Africa), Sci. Total Environ. 468–469 (2014) 584–597, https://doi.org/10.1016/j.scitotenv.2013.08.041.
[14] A. Colella, B. de Gennaro, S. Salvestrini, C. Colella, Surface interaction of humic acids with natural and synthetic phillipsite, J. Porous. Mater. 22 (2015) 501–509, https://doi.org/10.1007/s10934-015-9920-1.
[15] S. Canzano, S. Capasso, M. Di Natale, A. Erto, P. Iovino, D. Musmarra, Remediation of groundwater polluted by aromatic compounds by means of adsorption, Sustain 6 (2014) 4807–4822, https://doi.org/10.3390/su6084807.
[16] A. Erto, R. Andreozzi, F. Di Natale, A. Lancia, D. Musmarra, Experimental and isotherm-models analysis on TCE and PCE adsorption onto activated carbon, Chem. Eng. Trans. 17 (2009) 293–298, https://doi.org/10.3303/CET0917050.
[17] A. Erto, S. Chianese, A. Lancia, D. Musmarra, On the mechanism of benzene and toluene adsorption in single-compound and binary systems: energetic interactions and competitive effects, Desalin. Water Treat. 86 (2017) 259–265, https://doi.org/10.5004/dwt.2017.20712.
[18] S. Capasso, S. Salvestrini, V. Roviello, M. Trifuoggi, P. Iovino, Electrochemical removal of humic acids from water using aluminum anode: influence of chloride ion and current parameters, J. Chem. (2019) (2019) 1–6, https://doi.org/10.1155/2019/5401475.
[19] I. Michael, A. Achilleos, D. Lambropoulou, V.O. Torrens, S. Pérez, M. Petrović, D. Barceló, D. Fatta-Kassinos, Proposed transformation pathway and evolution profile of diclofenac and ibuprofen transformation products during (sono)photocatalysis, Appl. Catal. B Environ. 147 (2014) 1015–1027, https://doi.org/10.1016/j.apcatb.2013.10.035.
[20] P. Iovino, S. Chianese, S. Canzano, M. Prisciandaro, D. Musmarra, Degradation of ibuprofen in aqueous solution with UV light: the effect of reactor volume and pH, Water Air Soil Pollut. 227 (2016) 194, https://doi.org/10.1007/s11270-016-2890-3.
[21] M. Capocelli, M. Prisciandaro, A. Lancia, D. Musmarra, Modeling of cavitation as an advanced wastewater treatment, Desalin. Water Treat. 51 (2013) 1609–1614, https://doi.org/10.1080/19443994.2012.705094.
[22] M. Kovacic, J. Papac, H. Kusic, P. Karamanis, A. Loncaric Bozic, Degradation of polar and non-polar pharmaceutical pollutants in water by solar assisted photocatalysis using hydrothermal TiO2-SnS2, Chem. Eng. J. 382 (2020) 122826, , https://doi.org/10.1016/j.cej.2019.122826.
[23] S. Chianese, P. Iovino, V. Leone, D. Musmarra, M. Prisciandaro, Photodegradation of diclofenac sodium salt in water solution: effect of HA, NO < inf > 3 < /inf > ⁻and TiO < inf > 2 < /inf > on photolysis performance, Water Air Soil Pollut. 228 (2017), https://doi.org/10.1007/s11270-017-3445-y.
[24] E.M. Peña-Méndez, J. Havel, J. Patočka, Humic substance - Compounds of still unknown structure: applications in agriculture, industry, environment, and biomedicine, J. Appl. Biomed. 3 (2005) 13–24, https://doi.org/10.32725/jab.2005.002.
[25] P. Bartels, W. von Tümpling, Solar radiation influence on the decomposition process of diclofenac in surface waters, Sci. Total Environ. 374 (2007) 143–155, https://doi.org/10.1016/j.scitotenv.2006.11.039.
[26] P. Iovino, S. Chianese, S. Canzano, M. Prisciandaro, D. Musmarra, Photodegradation of diclofenac in wastewaters, Desalin. Water Treat. 61 (2017) 293–297, https://doi.org/10.5004/dwt.2016.11063.
[27] P. Iovino, S. Chianese, S. Canzano, M. Prisciandaro, D. Musmarra, Ibuprofen photodegradation in aqueous solutions, Environ. Sci. Pollut. Res. (2016), https://doi.org/10.1007/s11356-016-7339-0.
[28] D. Vogna, R. Marotta, A. Napolitano, R. Andreozzi, M. D'Ischia, Advanced oxidation of the pharmaceutical drug diclofenac with UV/H 2O2 and ozone, Water Res. 38 (2004) 414–422, https://doi.org/10.1016/j.watres.2003.09.028.
[29] B. Liu, S. gen Zhang, C.C. Chang, Emerging pollutants—part II: treatment, Water Environ. Res. 91 (2019) 1390–1401, https://doi.org/10.1002/wer.1233.
[30] P. Iovino, S. Chianese, M. Prisciandaro, D. Musmarra, Triclosan photolysis: operating condition study and photo-oxidation pathway, Chem. Eng. J. 377 (2019), https://doi.org/10.1016/j.cej.2019.02.132.
[31] L. Wu, C. Du, J. He, Z. Yang, H. Li, Effective adsorption of diclofenac sodium from neutral aqueous solution by low-cost lignite activated cokes, J. Hazard. Mater. 384 (2020) 121284, , https://doi.org/10.1016/j.jhazmat.2019.121284.
[32] X.X. Liang, A.M. Omer, Z. hong Hu, Y. guang Wang, D. Yu, X. kun Ouyang, Efficient adsorption of diclofenac sodium from aqueous solutions using magnetic amine-functionalized chitosan, Chemosphere 217 (2019) 270–278, https://doi.org/10.1016/j.chemosphere.2018.11.023.
[33] B.N. Bhadra, P.W. Seo, S.H. Jhung, Adsorption of diclofenac sodium from water using oxidized activated carbon, Chem. Eng. J. 301 (2016) 27–34, https://doi.org/10.1016/j.cej.2016.04.143.
[34] L. Lonappan, Y. Liu, T. Rouissi, S.K. Brar, R.Y. Surampalli, Development of biochar-based green functional materials using organic acids for environmental applications, J. Clean. Prod. 244 (2020) 118841, , https://doi.org/10.1016/j.jclepro.2019.118841.
[35] P. Iovino, S. Canzano, S. Capasso, A. Erto, D. Musmarra, A modeling analysis for the assessment of ibuprofen adsorption mechanism onto activated carbons, Chem. Eng. J. 277 (2015) 360–367, https://doi.org/10.1016/j.cej.2015.04.097.
[36] M. Taghdiri, N. Zamani, Hexamine adsorption study on activated carbon from aqueous solutions for application in treatment of hexamine industrial wastewater, Int J Environ Sci Technol. 10 (2013) 19–26, https://doi.org/10.1007/s13762-012-0102-2.
[37] S. Salvestrini, J. Jovanović, B. Adnadjević, Comparison of adsorbent materials for herbicide diuron removal from water, Desalin. Water Treat. 57 (2016) 22868–22877, https://doi.org/10.1080/19443994.2016.1180484.
[38] C. Moreno-Castilla, Adsorption of organic molecules from aqueous solutions on carbon materials, Carbon N Y. 42 (2004) 83–94, https://doi.org/10.1016/j.carbon.2003.09.022.
[39] L. Piai, M. Blokland, A. van der Wal, A. Langenhoff, Biodegradation and adsorption of micropollutants by biological activated carbon from a drinking water production plant, J. Hazard. Mater. 388 (2020) 122028, , https://doi.org/10.1016/j.jhazmat.2020.122028.
[40] S. Salvestrini, A modification of the Langmuir rate equation for diffusion-controlled adsorption kinetics, React Kinet Mech Catal. 128 (2019) 571–586, https://doi.org/10.1007/s11144-019-01684-9.
[41] Y.S. Ho, G. McKay, Pseudo-second order model for sorption processes, Process Biochem. 34 (1999) 451–465, https://doi.org/10.1016/S0032-9592(98)00112-5.
[42] H.P. Boehm, Surface oxides on carbon and their analysis: a critical assessment, Carbon 40 (2002) 145–149, https://doi.org/10.1016/S0008-6223(01)00165-8.
[43] A. Erto, R. Andreozzi, A. Lancia, D. Musmarra, Factors affecting the adsorption of trichloroethylene onto activated carbons, Appl. Surf. Sci. 256 (2010) 5237–5242, https://doi.org/10.1016/j.apsusc.2009.12.110.
[44] S. Salvestrini, P. Vanore, A. Bogush, S. Mayadevi, L.C. Campos, Sorption of metaldehyde using granular activated carbon, J. Water Reuse. Desalin. 7 (2017) 280–287, https://doi.org/10.2166/wrd.2016.074.
[45] J. Rivera-Utrilla, I. Bautista-Toledo, M.A. Ferro-Garca, C. Moreno-Castilla, Activated carbon surface modifications by adsorption of bacteria and their effect on aqueous lead adsorption, J. Chem. Technol. Biotechnol. 76 (2001) 1209–1215, https://doi.org/10.1002/jctb.506.
[46] D.B. França, P. Trigueiro, E.C. Silva Filho, M.G. Fonseca, M. Jaber, Monitoring diclofenac adsorption by organophilic alkylpyridinium bentonites, Chemosphere 242 (2020) 125109, https://doi.org/10.1016/j.chemosphere.2019.125109.
[47] J.M. Cabot, E. Fuguet, M. Rosés, Determination of acidity constants of sparingly soluble drugs in aqueous solution by the internal standard capillary electrophoresis method, Electrophoresis 35 (2014) 3564–3569, https://doi.org/10.1002/elps.201400353.
[48] R. Baccar, M. Sarrà, J. Bouzid, M. Feki, P. Blánquez, Removal of pharmaceutical compounds by activated carbon prepared from agricultural by-product, Chem. Eng. J. 211–212 (2012) 310–317, https://doi.org/10.1016/j.cej.2012.09.099.
[49] S. Rovani, M.T. Censi, S.L. Pedrotti, É.C. Lima, R. Cataluña, A.N. Fernandes, Development of a new adsorbent from agro-industrial waste and its potential use in endocrine disruptor compound removal, J. Hazard. Mater. 271 (2014) 311–320, https://doi.org/10.1016/j.jhazmat.2014.02.004.
[50] C. Saucier, M.A. Adebayo, E.C. Lima, R. Cataluña, P.S. Thue, L.D.T. Prola, M.J. Puchana-Rosero, F.M. Machado, F.A. Pavan, G.L. Dotto, Microwave-assisted activated carbon from cocoa shell as adsorbent for removal of sodium diclofenac and nimesulide from aqueous effluents, J. Hazard. Mater. 289 (2015) 18–27, https://doi.org/10.1016/j.jhazmat.2015.02.026.
[51] J.R. Domínguez, T. González, P. Palo, E.M. Cuerda-Correa, Removal of common pharmaceuticals present in surface waters by Amberlite XAD-7 acrylic-ester-resin: influence of pH and presence of other drugs, Desalination 269 (2011) 231–238, https://doi.org/10.1016/j.desal.2010.10.065.
[52] Y. Zhao, C.W. Cho, D. Wang, J.W. Choi, S. Lin, Y.S. Yun, Simultaneous scavenging of persistent pharmaceuticals with different charges by activated carbon fiber from aqueous environments, Chemosphere 247 (2020) 125909, , https://doi.org/10.1016/j.chemosphere.2020.125909.
[53] V. Rakić, V. Rac, M. Krmar, O. Otman, A. Auroux, The adsorption of pharmaceutically active compounds from aqueous solutions onto activated carbons, J. Hazard. Mater. 282 (2015) 141–149, https://doi.org/10.1016/j.jhazmat.2014.04.062.
[54] Z. Hasan, N.A. Khan, S.H. Jhung, Adsorptive removal of diclofenac sodium from water with Zr-based metal–organic frameworks, Chem. Eng. J. 284 (2016) 1406–1413, https://doi.org/10.1016/j.cej.2015.08.087.
[55] M. Varga, M. ELAbadsa, E. Tatár, V.G. Mihucz, Removal of selected pharmaceuticals from aqueous matrices with activated carbon under batch conditions, Microchem. J. 148 (2019) 661–672, https://doi.org/10.1016/j.microc.2019.05.038.
[56] R. Guillossou, J. Le Roux, R. Mailler, C.S. Pereira-Derome, G. Varrault, A. Bressy, E. Vulliet, C. Morlay, F. Nauleau, V. Rocher, J. Gasperi, Influence of dissolved organic matter on the removal of 12 organic micropollutants from wastewater

effluent by powdered activated carbon adsorption, Water Res. 172 (2020) 115487, , https://doi.org/10.1016/j.watres.2020.115487.
[57] J. Margot, C. Kienle, A. Magnet, M. Weil, L. Rossi, L.F. de Alencastro, C. Abegglen, D. Thonney, N. Chèvre, M. Schärer, D.A. Barry, Treatment of micropollutants in municipal wastewater: Ozone or powdered activated carbon? Sci. Total Environ. 461–462 (2013) 480–498, https://doi.org/10.1016/j.scitotenv.2013.05.034.
[58] V. Kårelid, G. Larsson, B. Björlenius, Pilot-scale removal of pharmaceuticals in municipal wastewater: comparison of granular and powdered activated carbon treatment at three wastewater treatment plants, J. Environ. Manage. 193 (2017) 491–502, https://doi.org/10.1016/j.jenvman.2017.02.042.
[59] C. Sheng, A.G.A. Nnanna, Y. Liu, J.D. Vargo, Removal of Trace Pharmaceuticals from Water using coagulation and powdered activated carbon as pretreatment to ultrafiltration membrane system, Sci. Total Environ. 550 (2016) 1075–1083, https://doi.org/10.1016/j.scitotenv.2016.01.179.
[60] P. de P.J. (Autore) Atkins, J. de Paula, J. Keeler, Atkins' Physical Chemistry, 9th ed., OUP Oxford, Oxford, 2017.
[61] T. De Oliveira, R. Guégan, T. Thiebault, C. Le Milbeau, F. Muller, V. Teixeira, M. Giovanela, M. Boussafir, Adsorption of diclofenac onto organoclays: effects of surfactant and environmental (pH and temperature) conditions, J. Hazard. Mater. 323 (2017) 558–566, https://doi.org/10.1016/j.jhazmat.2016.05.001.
[62] P.V.S. Lins, D.C. Henrique, A.H. Ide, J.L. da silva Duarte, G.L. Dotto, A. Yazidi, L. Sellaoui, A. Erto, C.L. de Paiva e Silva Zanta, L. Meili, Adsorption of a non-steroidal anti-inflammatory drug onto MgAl/LDH-activated carbon composite – Experimental investigation and statistical physics modeling, Colloids Surf. A Physicochem Eng. Asp. 586 (2020) 124217, , https://doi.org/10.1016/j.colsurfa.2019.124217.
[63] N. Suriyanon, P. Punyapalakul, C. Ngamcharussrivichai, Mechanistic study of diclofenac and carbamazepine adsorption on functionalized silica-based porous materials, Chem. Eng. J. 214 (2013) 208–218, https://doi.org/10.1016/j.cej.2012.10.052.
[64] N.T.M. Tam, Y. Liu, H. Bashir, Z. Yin, Y. He, X. Zhou, Efficient removal of diclofenac from aqueous solution by potassium ferrate-activated porous graphitic biochar: ambient condition influences and adsorption mechanism, Int. J. Environ. Res. Public Health 17 (2020) 291, https://doi.org/10.3390/ijerph17010291.
[65] A. Fenti, P. Iovino, S. Salvestrini, Some remarks on "A critical review of the estimation of the thermodynamic parameters on adsorption equilibria. Wrong use of equilibrium constant in the Van't hoof equation for calculation of thermodynamic parameters of adsorption", J. Molecular L J. Mol. Liq. 276 (2019) 529–530, https://doi.org/10.1016/j.molliq.2018.12.019.
[66] S. Canzano, P. Iovino, S. Salvestrini, S. Capasso, Comment on "Removal of anionic dye Congo red from aqueous solution by raw pine and acid-treated pine cone powder as adsorbent: equilibrium, thermodynamic, kinetics, mechanism and process design,", Water Res. 46 (2012) 4314–4315, https://doi.org/10.1016/j.watres.2012.05.040.
[67] S. Salvestrini, V. Leone, P. Iovino, S. Canzano, S. Capasso, Considerations about the correct evaluation of sorption thermodynamic parameters from equilibrium isotherms, J. Chem. Thermodyn. 68 (2014) 310–316, https://doi.org/10.1016/j.jct.2013.09.013.
[68] A. Fenti, S. Salvestrini, Analytical solution of the Langmuir-based linear driving force model and its application to the adsorption kinetics of boscalid onto granular activated carbon, React Kinet Mech Catal. 125 (2018) 1–13, https://doi.org/10.1007/s11144-018-1435-8.
[69] D. Robati, Pseudo-second-order kinetic equations for modeling adsorption systems for removal of lead ions using multi-walled carbon nanotube, J. Nanostructure Chem. 3 (2013) 55, https://doi.org/10.1186/2193-8865-3-55.
[70] J.P. Simonin, On the comparison of pseudo-first order and pseudo-second order rate laws in the modeling of adsorption kinetics, Chem. Eng. J. 300 (2016) 254–263, https://doi.org/10.1016/j.cej.2016.04.079.
[71] K.V. Kumar, Pseudo-second order models for the adsorption of safranin onto activated carbon: comparison of linear and non-linear regression methods, J. Hazard. Mater. 142 (2007) 564–567, https://doi.org/10.1016/j.jhazmat.2006.08.018.
[72] S. Salvestrini, S. Canzano, P. Iovino, V. Leone, S. Capasso, Modelling the biphasic sorption of simazine, imidacloprid, and boscalid in water/soil systems, J. Environ. Sci. Heal - Part B Pestic. Food Contam. Agric. Wastes. 49 (2014) 578–590, https://doi.org/10.1080/03601234.2014.911575.
[73] Y.H. Li, Z. Di, J. Ding, D. Wu, Z. Luan, Y. Zhu, Adsorption thermodynamic, kinetic and desorption studies of Pb2+ on carbon nanotubes, Water Res. 39 (2005) 605–609, https://doi.org/10.1016/j.watres.2004.11.004.
[74] Y. Xiao, J. Azaiez, J.M. Hill, Erroneous application of pseudo-second-Order adsorption kinetics model: ignored assumptions and spurious correlations, Ind. Eng. Chem. Res. 57 (2018) 2705–2709, https://doi.org/10.1021/acs.iecr.7b04724.
[75] S. Canzano, P. Iovino, V. Leone, S. Salvestrini, S. Capasso, Use and misuse of sorption kinetic data: a common mistake that should be avoided, Adsorp. Sci. Technol. 30 (2012) 217–225, https://doi.org/10.1260/0263-6174.30.3.217.
[76] S. Chianese, A. Fenti, P. Iovino, D. Musmarra, S. Salvestrini, Sorption of organic pollutants by humic acids: a review, Molecules 25 (2020) 918, https://doi.org/10.3390/molecules25040918.
[77] J. Cranck, The Mathematics of Diffusion, second, Claredon Press, Oxford, 1975.
[78] S. Salvestrini, Analysis of the Langmuir rate equation in its differential and integrated form for adsorption processes and a comparison with the pseudo first and pseudo second order models, React Kinet Mech Catal. 123 (2018) 455–472, https://doi.org/10.1007/s11144-017-1295-7.
[79] T.R. Waite, Bimolecular reaction rates in solids and liquids, J. Chem. Phys. 32 (1960) 21–23, https://doi.org/10.1063/1.1700904.
[80] M. Haerifar, S. Azizian, Mixed surface reaction and diffusion-controlled kinetic model for adsorption at the solid/solution interface, J Phys Chem C. 117 (2013) 8310–8317, https://doi.org/10.1021/jp401571m.
[81] J.S. Piccin, T.R.S. Cadaval, L.A.A. de Pinto, G.L. Dotto, Adsorption isotherms in liquid phase: experimental, modeling, and interpretations, Adsorpt Process Water Treat Purif, Springer International Publishing, Cham, 2017, pp. 19–51, https://doi.org/10.1007/978-3-319-58136-1_2.
[82] S. Salvestrini, Diuron herbicide degradation catalyzed by low molecular weight humic acid-like compounds, Environ. Chem. Lett. 11 (2013) 359–363, https://doi.org/10.1007/s10311-013-0415-5.
[83] P. Banerjee, S. Yashonath, B. Bagchi, Rotation driven translational diffusion of polyatomic ions in water: a novel mechanism for breakdown of Stokes-Einstein relation, J. Chem. Phys. 146 (2017) 164502, , https://doi.org/10.1063/1.4981257.